



Impact of Ni/Ge/Au/Ti/Au and Ti/Pt/Au collector metal on GaInP/GaAs HBT characteristics

Jae-Woo Park, Saeed Mohammadi, Dimitris Pavlidis *

Department of Electrical Engineering and Computer Science, The University of Michigan, 2307 EECS Building, 1301 Beal Avenue, Ann Arbor, MI 48109-2122, USA

Received 29 November 1999; accepted 26 January 2000

Abstract

The collector–emitter offset voltage of GaInP/GaAs HBTs grown by chemical-beam epitaxy with reduced toxicity precursors is investigated for Ni/Ge/Au/Ti/Au and Ti/Pt/Au collector contact metals. The offset voltage for HBTs with Ti/Pt/Au collector metal is increased by 0.26 V compared to Ni/Ge/Au/Ti/Au due to the 0.26 eV barrier existing between the n-GaAs subcollector and the Ti/Pt/Au contact metal. Other parameters affected by the collector contact barrier and impacting transistor performance include DC gain, microwave and power performance. © 2000 Elsevier Science Ltd. All rights reserved.

1. Introduction

GaInP/GaAs HBTs are considered a good alternative to AlGaAs/GaAs HBTs due to their large etching selectivity between the GaInP emitter and GaAs base which facilitates manufacturing and aluminum-free design which can be beneficial for improved reliability operation. The advantages of GaInP/GaAs over AlGaAs/GaAs-based HBT technology are supported by various reports on discrete device performance [1–4], and also on integrated circuits such as high-gain (18.8 dB, 52 dBΩ), broad-bandwidth (19 GHz) transimpedance amplifiers [5,6]. The presence of collector–emitter offset voltage (V_{offset}) impacts the HBT characteristics [7] and is of prime importance, in modern wireless applications where low voltage supply and high power-added-efficiency are key requirements. A possible way to reduce (V_{offset}) is by making use of double HBT (DHBT) design [8,9]. The collector and emitter contact metals are also affecting the offset voltage. In case of emitter contacts, the use of highly doped n-InGaAs allows significant reduction in emitter access resistance. This approach

cannot, however, be implemented for reducing the collector resistance (R_C) due to lattice mismatch between InGaAs and GaAs. Alloyed AuGeNi is usually employed as collector metal in GaAs-based devices. However, nonalloyed contacts such as Ti/Pt/Au provide more reproducible and uniform characteristics [10]. Ti/Pt/Au can present good ohmic characteristics when used as subcollector contact provided that it is deposited on highly doped n-GaAs. This approach allows ohmic behavior by tunneling despite the fact that the tunneling despite the fact that the metal work function of Ti is much higher than that of n-GaAs.

This paper reports the way that the offset voltage is influenced by the choice of different collector metals in case of HBTs with low-doped subcollector designs ($2\text{--}6 \times 10^{18} \text{ cm}^{-3}$). Experimental and theoretical investigations are conducted for this purpose and the (V_{offset}) dependence on collector metal barrier is discussed.

2. Device processing and characteristics

The GaInP/GaAs HBT wafers were grown by reduced-toxicity chemical-beam epitaxy (CBE). Ti/Pt/Au metal was first deposited on the InGaAs emitter cap which was doped at $1 \times 10^{19} \text{ cm}^{-3}$ and the emitter layer was subsequently etched to allow self-aligned base

* Corresponding author. Tel.: +1-734-6471778; fax: +1-734-7639324.

E-mail address: pavlidis@umich.edu (D. Pavlidis).

contact formation. NH₄OH and HCl-based solutions were used for etching of the GaAs and GaInP emitter layers respectively. Pt/Ti/Pt/Au was used for the base as this permitted minimum base contact resistance. A laterally etched undercut (LEU) process was developed and applied at the base and collector region to reduce base–collector capacitance (*C*_{BC}) while avoiding base resistance degradation [11]. Collector contacts using different metals were finally deposited. The wafers were diced into two pieces and two different metals, namely Ni/Ge/Au/Ti/Au (250/320/650/500/3000 Å) (HBT A) and Ti/Pt/Au (500/500/4000 Å) (HBT B) were deposited on the collector. Typical *I*–*V* characteristics for the two types of devices are shown in Fig. 1. The collector–emitter offset voltage was found to be shifted by ~0.26 V for HBT B with Ti/Pt/Au collector metal (*V*_{offset} = 0.51 V) compared to HBT A with Ni/Ge/Au/Ti/Au (*V*_{offset} = 0.25 V). The DC gain (*β* = 140) for HBT B is also lower than for HBT A (*β* = 180). To analyze these phenomena, the subcollector doping concentration was extracted using TLM patterns and the E–B and B–C junction diode characteristics were evaluated for the different metal schemes. Comparisons of the *V*_{offset} values as obtained directly from *I*–*V* characteristics were then performed to investigate the impact of metallization choice due to differences in E–B and B–C junctions.

3. Model for the collector–emitter offset voltage (*V*_{offset})

The collector–emitter offset voltage is defined as the difference between the turn-on voltage of the emitter–base (E–B) and the base–collector (B–C) junctions.

$$V_{\text{offset}} = V_{\text{BE}} - V_{\text{BC}} \text{ at } I_C = 0 \text{ mA.} \tag{1}$$

The collector current (*I*_C) is expressed using the Ebers–Moll equation as follows:

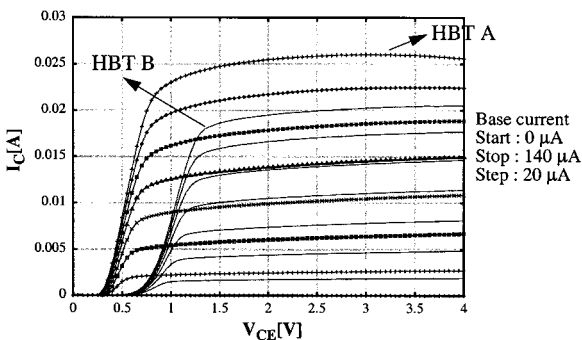


Fig. 1. *I*–*V* characteristics of 2 × 30 μm² self-aligned GaInP/GaAs HBTs with Ni/Ge/Au/Ti/Au (HBT A) and Ti/Pt/Au (HBT B).

$$I_C = \alpha_F A_E J_{ES} \exp[q(V_{\text{BE}} - I_E R_E - I_B R_B)/k_B T] - A_C J_{CS} \exp[q(V_{\text{BC}} - I_C R_C - I_B R_B)/k_B T] \tag{2}$$

where *R*_E, *R*_B, *R*_C are emitter, base and collector series resistances, *J*_{ES}, *J*_{CS} are emitter and collector saturation current densities, *I*_B, *I*_E are the base and emitter currents, *A*_E, *A*_C are emitter and collector areas and α_F is the forward current transfer factor.

*V*_{offset} can be obtained by setting *I*_C = 0 mA, [7,9] in Eq. (2) and solving *V*_{offset} as defined by Eq. (1). This leads to the following expression:

$$V_{\text{offset,ce}} = R_E I_B + \frac{k_B T}{q} \ln\left(\frac{A_C}{A_E}\right) + \frac{k_B T}{q} \ln\left(\frac{J_{CS}}{\alpha_F J_{ES}}\right). \tag{3}$$

For the case where an additional barrier of *qφ*_B = *q(φ*_S – χ) (where φ_B metal–semiconductor barrier height, φ_S is metal work function and χ is the electron affinity) exists between the n-GaAs collector and the collector metal, the modified Ebers–Moll model is provided in Fig. 2 and the corresponding collector current equation is given by:

$$I_C = \alpha_F A_E J_{ES} \exp[q(V_{\text{BE}} - I_E R_E - I_B R_B)/k_B T] - [A_C J'_{CS} \exp[q(V'_{\text{BC}} - I_C R_C - I_B R_B)/k_B T]] + A_C J_{CS} \exp[q\phi_B/k_B T], \tag{4}$$

where *V'*_{BC} = *V*_{BC} – φ_B and *J'*_{CS} is the collector saturation current density in case of thermionic emission at the collector metal barrier. This modified equation for the offset voltage can be found from Eq. (4) at *I*_C = 0:

$$V'_{\text{offset,ce}} \approx \phi_B + R_E I_B + \frac{k_B T}{q} \ln\left(\frac{A_C}{A_E}\right) + \frac{k_B T}{q} \ln\left(\frac{J'_{CS}}{\alpha_F J_{ES}}\right). \tag{5}$$

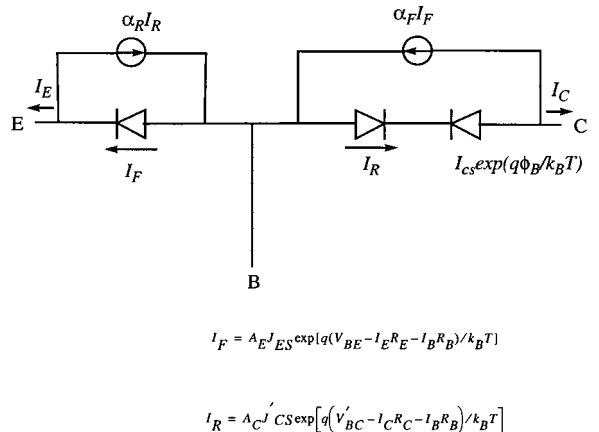


Fig. 2. The modified Ebers–Moll diagram with the collector metal barrier.

The above equation will be used as a basis of the analysis performed in Section 4 in order to understand the impact of metal type on HBT performance.

4. DC characteristics

Four point probe measurements were performed on TLM patterns deposited on the various HBT layers (E, B and C) to allow metal/semiconductor contact evaluation. In the case of Ti/Pt/Au metals, it was not possible to extract the contact resistance due to the Schottky nature of the contact. In case of Ni/Ge/Au/Ti/Au metal, the metal–semiconductor characteristics were ohmic and the evaluated contact parameters were $R_C = 3.2 \Omega$ (contact resistance), $R_S = 37.5 \Omega \text{ sq}$ (layer sheet resistance) and $L_t = 6.38 \mu\text{m}$ (transfer length). The extracted subcollector doping concentration from TLM measurements was $5 \times 10^{18} \text{ cm}^{-3}$.

Fig. 3 shows the E–B and B–C junction diode characteristics. In case of the E–B junction (Fig. 3a), the turn-on voltages are identical ($V_{BE} = 1.25 \text{ V}$) since the same emitter and base metals are used and only the collector metallization is different. The B–C junction diode characteristics (Fig. 3b) manifest, however, a turn-on voltage (V_{BC}) for HBT B (1.75 V) which is 0.75 V larger than for HBT A (1.0 V). According to the theoretically predicted collector–emitter offset voltage (V_{offset}) of Eq. (1), $V_{BE} (1.25 \text{ V}) - V_{BC} (1.0 \text{ V})$ is expected to be 0.25 V for HBT A which agrees with the offset voltage predicted from the I – V characteristics of Fig. 1 (discussed in Section 3).

Fig. 4 shows the metal–semiconductor band diagram which can be used to analyze the V_{offset} characteristics for HBT B. Here a Schottky barrier is formed between n-GaAs ($q\chi = 4.07 \text{ eV}$) and metal (Ti, $q\phi_S = 4.33 \text{ eV}$) and a collector contact barrier height ($q\phi_B = q(\phi_S - \chi)$) is established which equals 0.26 eV. If the n-GaAs subcollector is heavily doped, the barrier does not behave as Schottky but presents ohmic characteristics due to tunneling effects. However, the extracted subcollector doping concentration ($5 \times 10^{18} \text{ cm}^{-3}$) is not sufficiently high to allow ohmic contact operation as also evidenced by the small tunneling probability of less than 10% estimated from the following equation [12]:

$$T(\eta) \approx \exp(-q\phi_B/E_{00}) = 0.09, \quad (6)$$

where

$$E_{00} = \frac{qh}{4\pi} \sqrt{\frac{N_D}{\epsilon_S m^*}} \quad (7)$$

and ϵ_S is the semiconductor permittivity (13.1), m^* is effective mass of GaAs (0.067), N_D is donor impurity density ($5 \times 10^{18} \text{ cm}^{-3}$) and ϕ_B is Schottky barrier height on n-type semiconductor (0.26 eV).

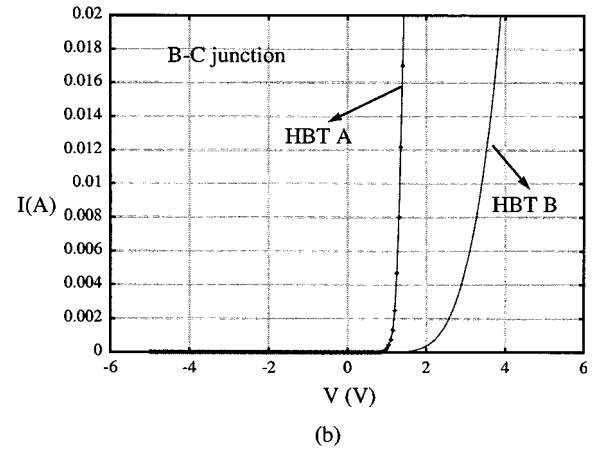
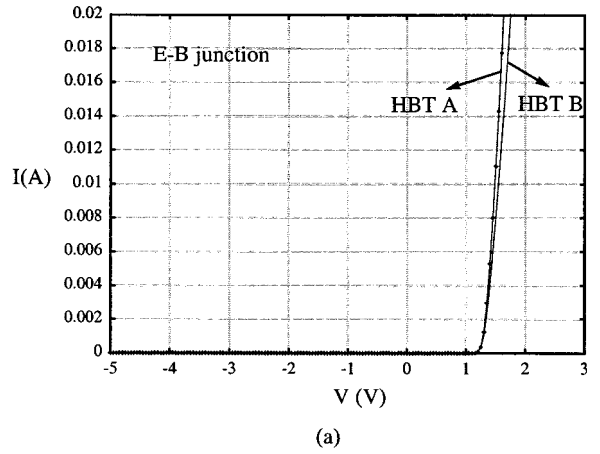


Fig. 3. (a) E–B and (b) B–C diode characteristics for different collector metals.

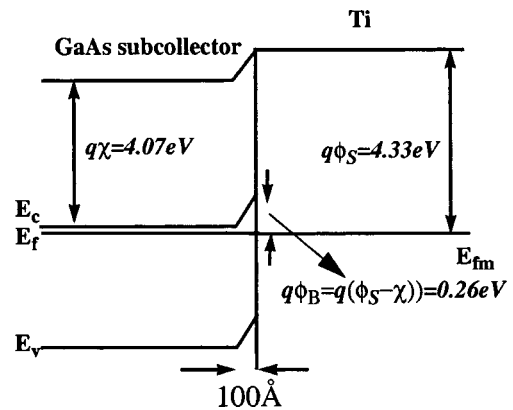


Fig. 4. Energy-band diagram for n-GaAs subcollector ($n = 5 \times 10^{18} \text{ cm}^{-3}$) and metal (Ti).

To achieve the same potential energy in the E–B and B–C junctions of the investigated GaInP/GaAs HBTs, the turn-on voltage (V_{BC}) should be 1.25 V so that it

equals V_{BE} . Thus, an additional 0.25 V bias is needed at the collector side to obtain a total V_{BC} value of 1.25 V for HBT A (Ni/Ge/Au/Ti/Au collector metal). In case of HBT B (Ti/Pt/Au collector metal), one needs to consider the additional Schottky barrier ($q\phi_B = 0.26$ V) in conjunction with the corresponding turn-on voltage, $V_{BC} = 1.0$ V. The combination of $V_{BC} = 1.0$ V and contact barrier (ϕ_B) of 0.26 V results in an effective V_{BC} value V'_{BC} value of 0.74 V. At least +0.51 V needs to be applied consequently under such circumstances to the collector in order to obtain a net V_{BC} value of 1.25 V which equals the base-emitter turn-on voltage. The obtained results are consequently consistent with the value of 0.51 V measured for V_{offset} of HBT B.

In summary, for a Schottky contact between n-GaAs and Ti metal (HBT B), the offset voltage is given by

$$\begin{aligned} V_{offset} &= V_{BE}(1.25 \text{ V n-GaInP/p-GaAs}) \\ &\quad - V_{BC}(1.0 \text{ V for p-GaAs/n-GaAs} \\ &\quad \quad - 0.26 \text{ V for Schottky barrier}) \\ &= 0.51 \text{ V.} \end{aligned}$$

By employing suitable values for the parameters of Eq. (5) ($\phi_B = 0.26$ V, $R_{E}I_B = 0.5$ mV, the third term of Eq. (5) = 0.1 V, the fourth term of Eq. (5) = 0.51 V), V_{offset} for HBT B was estimated to be 0.51 V which agrees with the value obtained from $V_{offset} = V_{BE} - V'_{BC}$. The potential barrier formed between the n-GaAs collector and the collector metal results in current blocking which impacts the total collector current (I_C). Thus, a modified total collector current equation in presence of a potential barrier as shown in Eq. (4) needs to be considered. Consideration of Fig. 2 showed that the barrier height (ϕ_B) affects the HBT saturation current I_S which in turn affects the $\alpha_F I_F$ current source ($\alpha_F I_S = \alpha_F A_E J_{ES}$) and as a result the total collector current (I_C) can be reduced for increased ϕ_B values. According to large signal model extraction using HSPICE, the extracted I_S is 6.26×10^{-23} and 4.76×10^{-23} for HBT A and HBT B, respectively. The calculated total collector current (at $V_{BE} = 1.4$ V, $V_{CE} = 2.5$ V) for HBT B using Eq. (4) is therefore found to be by 5 mA lower than HBT A which agrees with the measured total collector current for HBT B.

5. RF characteristics

The microwave properties of both HBT types measured in common-emitter configuration using on wafer tests and an HP8510B network analyzer. The power and current gain versus frequency characteristics of the HBTs with different collector metals are shown in Fig. 5. A comparison of microwave performance at same V_{CE} (3.5 V) and I_B (120 μ A) bias should ideally result in similar performance for HBT A and B if the same

collector metal is employed. The f_T and f_{max} values extracted from Fig. 5 employ therefore the same bias conditions (V_{CE} , I_B) so that the impact of collector metal can be investigated. The current gain cutoff frequency (f_T) extrapolated from the measured $|H_{21}|$ using the -6 dB/Oct. slope rule was 47 GHz for HBT A with Ni/Ge/Au/Ti/Au collector metal, and 42 GHz for HBT B with Ti/Pt/Au collector metal. The maximum oscillation frequency (f_{max}) from Mason's unilateral gain (U) was 65 GHz for the HBT A and 52 GHz for HBT B respectively. This corresponds to an f_T increase of 7% and f_{max} increase of 25% as a result of using Ni/Ge/Au/Ti/Au collector metal.

High-frequency small-signal equivalent circuit parameters of the GaInP/GaAs HBTs with different collector metals were extracted in an attempt to provide physical insight to the device by analyzing the obtained parameters [13]. The results are summarized in Table 1.

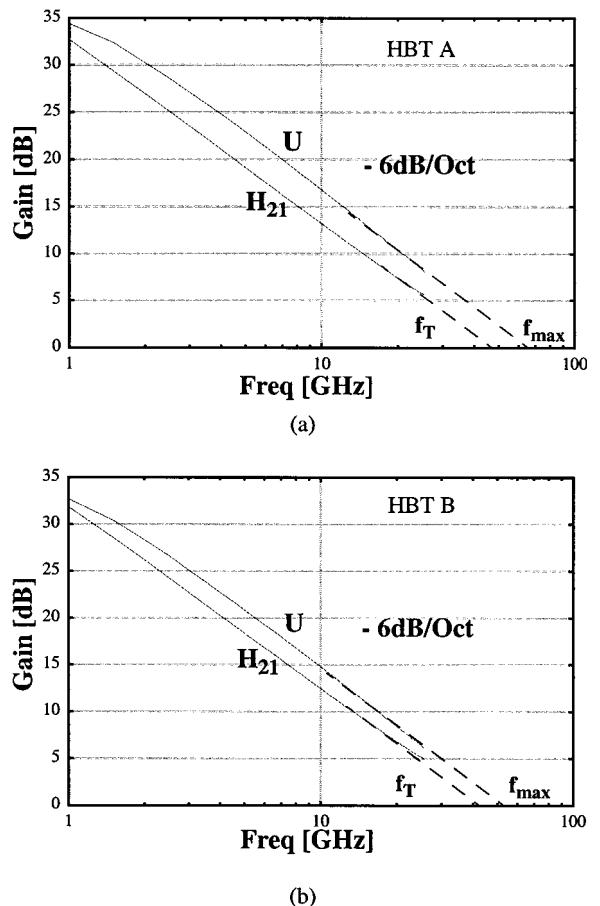


Fig. 5. Microwave performance of GaInP/GaAs HBTs with different collector metals ($V_{CE} = 3.5$ V, $I_B = 120$ μ A, $I_C = 19.5$ mA for HBT A, $V_{CE} = 3.5$ V, $I_B = 120$ μ A, $I_C = 14.1$ mA for HBTB).

Table 1

Equivalent circuit parameters for $2 \times 30 \mu\text{m}^2$ single emitter HBT between HBT A with Ni/Ge/Au/Ti/Au and HBT B with Ti/Pt/Au collector metal^a

Sample	R_B	R_{BE}	R_C	R_E	C_{BE}	C_{BC}	α_T	β	f_T/f_{max}	I_B	V_{CE}/I_C
HBT A with Ni/Ge/Au/Ti/Au	7.37	1.33	12.6	4.33	0.53	32	0.99	162	47/65	120	3.5/19.5
HBT B with Ti/Pt/Au	8.4	1.86	27.4	4.33	0.38	34	0.99	116	42/52	120	3.5/14.1

^a $R = \Omega$, $C = \text{fF}$, $\beta = \text{DC current gain}$, $I_B = \mu\text{A}$, $f_T/f_{\text{max}} = \text{GHz}$, $I_C = \text{mA}$, $V_{CE} = \text{V}$.

As expected, the collector resistance (R_C) for HBT A is much lower than for HBT B. This reflects the fact that the contact resistance is reduced when employing Ni/Ge/Au/Ti/Au. The intrinsic and access collector resistances impact significantly the total resistance due to the low subcollector doping $5 \times 10^{18} \text{ cm}^{-3}$ in both devices but the impact of contact resistance can still be seen in the measured total collector resistance values. Study of the small-signal equivalent circuit parameters, showed that the base-emitter resistance (R_{BE}) is reduced but the base-emitter capacitance (C_{BE}) of HBT A is increased due to the collector current (I_C) increase. As a result, the emitter transit time ($\tau_e = R_{BE} \times C_{BE}$) of HBT A has the same value as for HBT B, and the f_T values do not differ significantly. Since the collector current of HBT A is higher than for HBT B, the base resistance (R_B) of HBT A is reduced leading to improved maximum oscillation frequency ($f_{\text{max}} = 54 \text{ GHz}$) characterization. In summary, HBT B with Schottky barrier in the collector produces higher R_C and lower I_C due to current blocking in the Schottky barrier. Thus, R_B which is the function of I_C is increased and the maximum oscillation frequency (f_T) is reduced.

6. Power characteristics

The influence of different collector metals on the power characteristics was also studied. Fig. 6 shows the measured large signal output power (P_{out}) and power-added efficiency (PAE) as function of the RF input power for one finger $2 \times 30 \mu\text{m}^2$ devices. All HBTs were characterized under optimum bias, source and load impedance conditions for maximum output power under large signal operation at 8 GHz. The devices were biased for Class B ($V_{CE} = 7 \text{ V}$, $V_{BE} = 0.77 \text{ V}$) operation.

The input power was swept up to the 3 dB gain compression point while maintaining constant V_{CE} and V_{BE} bias. The output power (P_{out}), power gain (G) and the collector current of the HBT were recorded and PAE was evaluated. The HBT A with Ni/Ge/Au/Ti/Au collector metal produces higher output power as well as PAE compared to HBT B with Ti/Pt/Au collector metal. The maximum output power was 18.4 and 17.5 dBm for HBT A and HBT B respectively while the corresponding peak PAE as 63.1% and 51.2%. This indicates that the

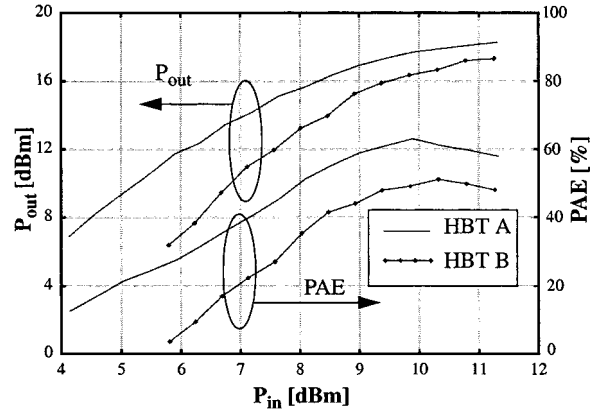


Fig. 6. $P_{\text{in}}-P_{\text{out}}$ of GaInP/GaAs HBTs with different collector metals.

larger power dissipation through the large R_C (Ti/Pt/Au collector contact) of HBT B affects its maximum output power performance. In particular, HBT A with Ni/Ge/Au/Ti/Au metal has lower knee voltage (V_k) which leads to an increased output power as a result of the imposed limits in V_k at I_{cmax} and V_{max} at $I_C = 0$ and higher DC gain compared to HBT B. Thus the small contact resistance of the HBT A with Ni/Ge/Au/Ti/Au collector metal leads to an improved power performance due to the resulting lower knee voltage and higher DC gain.

7. Conclusions

The importance of the collector metal choice in HBT DC, RF, power performance is reported. The presence of unintentional collector contact barrier leads to a change in the Ebers-Moll model predicted characteristics and affects the collector offset voltage due to the presence of barrier height ($q\phi_B = 0.26 \text{ V}$ for Ti/Pt/Au). As a result, the total collector current is reduced leading to a smaller DC gain ($\Delta\beta = 46$) for HBTs with Ti/Pt/Au collector metal. The RF and power performance of HBTs with Ti/Pt/Au is influenced by the presence of large R_C resulting from the presence of the collector contact barrier. The maximum output power for HBTs with Ni/Ge/Au/Ti/Au metal is 18.4 dBm while the peak PAE is 63.1%. This corresponds to improved power

characteristics compared with HBTs that present a Schottky barrier at the collector contact.

Acknowledgements

The authors would like to thank Jean-Charles Garcia and J.L. Guyaux, Thomson-CSF, Central Research Laboratory, for CBE growth and helpful discussions. This work was supported in part by Thomson-CSF (Contract No. 94 6M 917) and MURI (Contract No. DAAH04-96-1-0001).

References

- [1] Razeghi M, Omnes F, Defour M, Maurel P, Hu J, Pavlidis D. High performance GaAs/GaInP HBTs grown by MOCVD. *Sem Sci Tec* 1990;5:278–80.
- [2] Park J-W, Pavlidis D, Mohammadi S, Dua C, Garcia JC. Improved high frequency performance by composite emitter AlGaAs/GaInP HBTs fabricated using CBE. *Proceedings of 24th International Symposium On Compound Semiconductor*, San Diego, 1997. p. 439–42.
- [3] Fresina MT, Ahmari DA, Mares PJ, Hartmann QJ, Feng M, Stillman GE. High-speed, low-noise InGaP/GaAs HBTs. *IEEE Electron Dev Lett* 1995;16:540–1.
- [4] Mochizuki K, Ouchi K, Hirata K, Tanoue T, Oka T, Masuda H. Polycrystal isolation of InGaP/GaAs HBT's to reduce collector capacitance. *IEEE Electron Dev Lett* 1998;19(2):47–9.
- [5] Park J-W, Mohammadi S, Pavlidis D, Dua C, Guyaux J, Garcia JC. GaInP/GaAs HBT broadband monolithic transimpedance amplifiers and their high frequency small and large signal characteristics. *IEEE MTT-S International Microwave Symposium*, 1998. p. 39–42.
- [6] Mohammadi S, Park J-W, Pavlidis D, Dua C, Guyaux J, Garcia JC. High-gain GaInP/GaAs HBT monolithic transimpedance amplifier for high-speed optoelectronic receivers. *Proceedings of IEEE International Device Meeting (IEDM)*, 1998. p. 661–4.
- [7] Won T, Iyer S, Agarwala S, Morkoc H. Collector offset voltage of HBTs grown by MBE. *IEEE Electron Dev Lett* 1989;10(6):274–6.
- [8] Mazhari B, Gao GB, Morkoc H. Collector–emitter offset voltage in HBTs. *Solid-State Electron* 1991;34(3):315–21.
- [9] Chand N, Fischer R, Morkoc H. Collector–emitter offset voltage in AlGaAs/GaAs HBTs. *Appl Phys Lett* 1985;47(3):313–5.
- [10] Gueret P, Buchman P, Daetwyler K, Vettiger P. Resistance of very small area ohmic contacts on GaAs. *Appl Phys Lett* 1989;55(17):1735–7.
- [11] Park J-W, Pavlidis D, Mohammadi S, Guyaux JL, Garcia J. Material and processing technology for manufacturing of high speed, high reliability GaInP/GaAs HBT based ICs. *International Conference on GaAs Manufacturing Technology*, Vancouver, Canada, 1999. p. 173–6.
- [12] Sze SM. *Physics of semiconductor devices*. New York: Wiley Interscience; 1981. p. 264.
- [13] Pehlke D, Pavlidis D. Evaluation of the factors determining HBT high-frequency performance by direct analysis of S-parameter data. *IEEE Trans Microwave Theory Tech* 1992;40:2367–73.